© 2017. Published by The Company of Biologists Ltd | Journal of Experimental Biology (2017) 220, 2418-2425 doi:10.1242/jeb.156430

RESEARCH ARTICLE

Cone-like rhodopsin expressed in the all-cone retina of the colubrid pine snake as a potential adaptation to diurnality

Nihar Bhattacharyya[1], Benedict Darren[1], Ryan K. Schott[2], Vincent Tropepe[1,3,4] and Belinda S. W. Chang[1,2,4,*]

ABSTRACT

Colubridae is the largest and most diverse family of snakes, with visual systems that reflect this diversity, encompassing a variety of retinal photoreceptor organizations. The transmutation theory proposed by Walls postulates that photoreceptors could evolutionarily transition between cell types in squamates, but few studies have tested this theory. Recently, evidence for transmutation and rod-like machinery in an all-cone retina has been identified in a diurnal garter snake (*Thamnophis*), and it appears that the rhodopsin gene at least may be widespread among colubrid snakes. However, functional evidence supporting transmutation beyond the existence of the rhodopsin gene remains rare. We examined the all-cone retina of another colubrid, *Pituophis melanoleucus*, thought to be more secretive/burrowing than *Thamnophis*. We found that *P. melanoleucus* expresses two cone opsins (SWS1, LWS) and rhodopsin (RH1) within the eye. Immunohistochemistry localized rhodopsin to the outer segment of photoreceptors in the all-cone retina of the snake and all opsin genes produced functional visual pigments when expressed *in vitro*. Consistent with other studies, we found that *P. melanoleucus* rhodopsin is extremely blue-shifted. Surprisingly, *P. melanoleucus* rhodopsin reacted with hydroxylamine, a typical cone opsin characteristic. These results support the idea that the rhodopsin-containing photoreceptors of *P. melanoleucus* are the products of evolutionary transmutation from rod ancestors, and suggest that this phenomenon may be widespread in colubrid snakes. We hypothesize that transmutation may be an adaptation for diurnal, brighter-light vision, which could result in increased spectral sensitivity and chromatic discrimination with the potential for colour vision.

KEY WORDS: Rod and cone photoreceptors, Photoreceptor transmutation, Rhodopsin, Visual pigments, Visual evolution, Reptile vision

INTRODUCTION

Reptiles are known for their impressive array of visual adaptations and retinal organizations, which reflect distinct ecologies and evolutionary histories (Underwood, 1970; Walls, 1942). The family Colubridae is the most speciose family of snakes and encompasses a diverse range of lifestyles and ecologies. Colubrid snakes have recently emerged as a compelling group in which to study visual system evolution and adaptation (Schott et al., 2016; Simões et al., 2015, 2016).

In the vertebrate retina, photoreceptor cells can be divided into two types based on their overall structure and function: cones, which are active in bright light and contain cone visual pigments (SWS1, SWS2, RH2, LWS) in a tapered outer segment, and rods, which function in dim light and contain rhodopsin (RH1) in a longer, more cylindrical outer segment (Bowmaker, 2008; Lamb, 2013; Walls, 1942). Reptilian retinas are unique in having multiple retinal configurations (Underwood, 1970) among closely related species, including all-rod (Kojima et al., 1992), rod and cone (Sillman et al., 2001), and all-cone (Sillman et al., 1997). In 1942, physiologist Gordon Walls outlined his theory of transmutation to explain the evolutionary transformation of photoreceptors from one type to another (Walls, 1942). This phenomenon has since been investigated in nocturnal geckos, where cone opsins are expressed in an all-rod retina in order to compensate for the evolutionary loss of RH1 in a hypothesized diurnal, all-cone ancestor (Kojima et al., 1992; Taniguchi et al., 1999). Although the nocturnal henophedian snakes, such as boas and pythons, are known to have duplex retinas expressing RH1, LWS and SWS1 in canonical photoreceptors (Davies et al., 2009), the more derived diurnal colubrid snakes have been primarily shown to posses simplex retinas comprising all-cone photoreceptors, with the fate of the rod photoreceptor unknown (Caprette, 2005; Underwood, 1970; Walls, 1942). Early studies of the colubrid visual system found a green-sensitive visual pigment in addition to a red and a blue pigment (Sillman et al., 1997) in the simplex retina, but were unable to distinguish between a spectrally shifted rhodopsin in a transmuted rod or a potentially resurrected RH2 cone opsin (Cortesi et al., 2015). More recently, a study from our group identified a functional blue-shifted RH1 pigment in the all-cone retina of the ribbon snake (*Thamnophis proximus*), and proposed that this resulted from a rod to cone evolutionary transmutation in colubrid snakes that may have allowed for enhanced spectral discrimination and even trichromatic colour vision (Schott et al., 2016). A recent study that sequenced the opsins of several other colubrid snake species discovered the widespread presence of full-length rhodopsin genes in species with supposed simplex retinas that were previously presumed to have lost rods or rhodopsins (Simões et al., 2016). However, detailed characterizations of colubrid snake opsins and photoreceptors in the context of the theory of evolutionary transmutation still remain rare.

To further test the hypothesis of widespread transmutation in colubrid snakes, and its potential functional consequences, we examined the visual system of the northern pine snake [*Pituophis melanoleucus* (Daudin 1803)], a diurnal colubrid snake distantly related to *T. proximus*. *Pituophis melanoleucus* inhabits the eastern half of the United States and Canada (Stull, 1940) and spends relatively short intervals on the surface during the day to forage for prey such as small mammals and birds, and to create new burrows

[1]Department of Cell & Systems Biology, University of Toronto, Toronto, Ontario, Canada M5S 3G5. [2]Department of Ecology & Evolutionary Biology, University of Toronto, Toronto, Ontario, Canada M5S 3B2. [3]Department of Ophthalmology & Vision Sciences, University of Toronto, Toronto Ontario, Canada M5T 3A9. [4]Centre for the Analysis of Genome Evolution and Function, University of Toronto, Toronto, Ontario, Canada M5S 3B2.

*Author for correspondence (belinda.chang@utoronto.ca)

B.S.W.C., 0000-0002-6525-4429

Received 16 January 2017; Accepted 13 April 2017

Journal of Experimental Biology

Journal of Experimental Biology (2017) 220, 2418-2425 doi:10.1242/jeb.156430

(Diller and Wallace, 1996; Himes, 2001). While *P. melanoleucus* has been found to possess an all-cone retina (Caprette, 2005), similar to previous diurnal colubrid snakes studied (Schott et al., 2016; Sillman et al., 1997), unlike other strongly diurnal colubrids such as the garter snake, *P. melanoleucus* is more secretive and is thought to spend a considerable amount of time burrowing (Gerald et al., 2006).

In this study, we investigate whether there is evidence of photoreceptor transmutation from rods into cones in the all-cone retina of *P. melanoleucus* via functional characterization, cellular localization and molecular evolutionary analyses of its visual pigment (opsin) genes. We isolated three opsin genes from *P. melanoleucus*: SWS1, LWS and RH1. Immunohistochemistry of the retina localized rhodopsin (RH1) protein and rod transducin to the inner and outer segments of a small subset of photoreceptors, suggesting that *P. melanoleucus* exemplifies another rod-to-cone transmutation in diurnal colubrids. All three opsins were successfully expressed *in vitro* and displayed properties characteristic of fully functional visual pigments. Additionally, spectroscopic assays revealed that *P. melanoleucus* rhodopsin is sensitive to hydroxylamine, which is more typical of cone opsins and is suggestive of more cone-like functional properties. This study provides further evidence for a fascinating evolutionary transformation in the retinas of colubrid snakes, with implications for reptiles in general.

MATERIALS AND METHODS

Animals

A northern pine snake (*Pituophis melanoleucus melanoleucus*, adult) specimen and mice (*Mus musculus*, adult, CD1) were obtained from a licensed source as commissioned by the University of Toronto Animal Care Committee. The specimen was euthanized using an approved protocol. The eyes were enucleated and preserved in RNAlater or 4% paraformaldehyde.

Total RNA extraction and cDNA synthesis

The dissected whole eye was homogenized with TRIzol, and total RNA was isolated using a phenol/chloroform extraction and ethanol precipitation. The first strand of complementary DNA (cDNA) was synthesized using SuperScript III Reverse Transcriptase (Invitrogen, Waltham, MA, USA) from RNA samples primed with a 3′ oligo-dT and a 5′ SMART primer, following the protocol outlined by the SMART cDNA Library Construction Kit (BD Biosciences, Franklin Lakes, NJ, USA). The second strand complement was synthesized by long-distance PCR following the same protocol.

Visual pigment genes were isolated using a degenerate PCR strategy. Degenerate primers based on an alignment of reptilian visual pigment sequences were used in attempts to amplify partial sequences of the LWS, SWS1 and RH1 opsin genes with a heminested strategy. GenomeWalker (Clontech, Mountain View, CA, USA) was additionally used to obtain full-length sequences (Table S1). Extracted PCR products were ligated into the pJET1.2 blunt plasmid vector.

Phylogenetic analysis

A representative set of vertebrate visual opsin sequences was obtained from GenBank. These sequences were combined with the three opsin genes sequenced from the pine snake and aligned using MUSCLE (Edgar, 2004). The poorly aligned 5′ and 3′ ends of the sequence were manually trimmed. Species list and accession numbers for all sequences used in the study are provided in Table S2. In order to confirm the identities of the opsin genes from the pine snake, a gene tree was estimated using the resulting alignment in MrBayes 3 (Ronquist and Huelsenbeck, 2003) using reversible jump MCMC with a gamma rate parameter (nst=mixed, rates=gamma), which explores the parameter space for the nucleotide model and the phylogenetic tree simultaneously. The analyses were run for five million generations with a 25% burn-in. Convergence was confirmed by checking that the standard deviations of split frequencies approached zero and that there was no obvious trend in the log likelihood plot.

Protein expression

Full-length opsin sequences (RH1, SWS1 and LWS) were amplified from pJET1.2 vector using primers that added the *Bam*HI and *Eco*RI restriction sites to its 5′ and 3′ ends, respectively, and inserted into the p1D4-hrGFP II expression vector (Morrow and Chang, 2010). Expression vectors containing *P. melanoleucus* cone opsin and rhodopsin genes were transiently transfected into cultured HEK293T cells (ATCC CRL-11268) using Lipofectamine 2000 (Invitrogen; 8 µg of DNA per 10-cm plate) and harvested after 48 h. Visual pigments were regenerated with 11-*cis* retinal, generously provided by Dr Rosalie Crouch (Medical University of South Carolina), solubilized in 1% dodecylmaltoside, and purified with the 1D4 monoclonal antibody (University of British Columbia 95-062, lot 1017; Molday and MacKenzie, 1983) as previously described (Morrow and Chang, 2015, 2010; Morrow et al., 2011). RH1 and SWS1 pigments were purified in sodium phosphate buffers and LWS was purified in HEPES buffers containing glycerol (as described in van Hazel et al., 2013). The ultraviolet-visible absorption spectra of purified visual pigments were recorded using a Cary 4000 double beam spectrophotometer (Agilent, Santa Clara, CA, USA). Dark-light difference spectra were calculated by subtracting light-bleached absorbance spectra from respective dark spectra. Pigments were photoexcited with light from a fiber optic lamp (Dolan-Jenner, Boxborough, MA, USA) for 60 s at 25°C. Absorbance spectra for acid bleach and hydroxylamine assays were measured following incubation in hydrochloric acid (100 mmol l^{-1}) and hydroxylamine (NH_2OH, 50 mmol l^{-1}), respectively. To estimate the wavelength of maximum absorption (λ_{max}), the dark absorbance spectra were baseline corrected and fit to Govardovskii templates for A1 visual pigments (Govardovskii et al., 2000).

Immunohistochemistry

Fixation of pine snake eyes was conducted as previously described (Schott et al., 2016). Briefly, after enucleating *P. melanoleucus* eyes in the light, they were rinsed in PBS (0.8% NaCl, 0.02% KCl, 0.144% $NaHPO_4$, and 0.024% KH_2PO_4, pH 7.4), fixed overnight at 4°C in 4% paraformaldehyde, infiltrated with increasing concentrations of sucrose (5%, 13%, 18%, 22%, 30%) in PBS, and embedded in a 2:1 solution of 30% sucrose and OCT compound (Tissue-Tek, Burlington, NC, USA) at −20°C. The eyes were cryosectioned transversely at −25°C in 20 µm sections using a Leica CM3050 (Wetzlar, Germany) cryostat, placed onto positively charged microscope slides, and stored at −80°C until use.

Slides were first rehydrated in PBS and then air-dried to ensure adhesion. Sections were rinsed three times in PBS with 0.1% Tween-20 (PBT) and then incubated in 4% paraformaldehyde PBS for 20 min. After rinsing in PBT and PDT (PBT with 0.1% DMSO), the slides were incubated in a humidity chamber with blocking solution (1% BSA in PDT with 2% normal goat serum) for 1 h, incubated with primary antibody diluted in blocking solution overnight at 4°C in a humidity chamber. Antibodies used were the

Journal of Experimental Biology (2017) 220, 2418-2425 doi:10.1242/jeb.156430

K20 antibody (Santa Cruz Biotechnology, Santa Cruz, CA, USA, sc-389, lot C1909, dilution: 1:500) and the RET-P1 anti-rhodopsin antibody (Sigma-Aldrich, St Louis, MO, USA, O-4886, lot 19H4839, dilution: 1:200).

After extensive rinsing and soaking in PDT (three times for 15 min), secondary antibody was added to the samples and incubated at 37°C for 1 h in a humidity chamber. Secondary antibodies used for the fluorescent staining were the AlexaFluor-488 anti-rabbit antibody (Life Technologies, Waltham, MA, USA, A11034, lot 1298480, dilution: 1:1000) and the Cy-3 anti-mouse antibody (Jackson ImmunoResearch, West Grove, PA, USA, 115-165-003, dilution: 1:800). After rinsing with PBS, followed by PDT, sections were stained with 10 µg ml^{-1} Hoechst for 10 min at room temperature. The sections were then rinsed in PBS and PDT and mounted with ProLong® Gold antifade reagent (Life Technologies) and cover-slipped. Sections were visualized via a Leica SP-8 confocal laser microscope.

RESULTS

Full-length RH1, SWS1 and LWS opsin sequences found in *Pituophis melanoleucus* cDNA

To determine the identities of the visual pigments in *P. melanoleucus*, eye cDNA and gDNA were screened for opsin genes. Three full-length opsins were amplified, sequenced and analyzed phylogenetically with a set of representative vertebrate visual opsins (Table S1) using Bayesian inference (MrBayes 3.0) (Ronquist and Huelsenbeck, 2003). This analysis confirmed the identity of the three opsin genes as RH1, LWS and SWS1 (Figs S1–S3).

All three opsin gene sequences contained the critical amino acid residues required for proper structure and function of a prototypical opsin, including K296, the site of the Schiff base linkage with 11-*cis* retinal (Palczewski et al., 2000; Sakmar et al., 2002), and E113, the counter-ion to the Schiff base in the dark state (Sakmar et al., 1989), as well as C110 and C187, which form a critical disulfide bond in the protein (Karnik and Khorana, 1990). Both cone opsin genes also have the conserved P189 residue, which is critical for faster cone opsin pigment regeneration (Kuwayama et al., 2002).

Interestingly, *P. melanoleucus* RH1 has serine at site 185 instead of the highly conserved cysteine, similar to several other snakes (Schott et al., 2016; Simões et al., 2016). Mutations at site 185 have been shown to reduce both visual pigment stability (McKibbin et al., 2007) and transducin activation *in vitro* (Karnik et al., 1988). Also, the *P. melanoleucus* RH1 has N83 and S292, which are often found in rhodopsins with blue-shifted λ_{max} values, and can also affect all-*trans* retinal release kinetics following photoactivation (Bickelmann et al., 2012; van Hazel et al., 2016).

Based on known spectral tuning sites in LWS, *P. melanoleucus* has A285, compared with T285 in *Thamnophis* snakes. T285A is known to blue-shift the LWS pigment by 16–20 nm (Asenjo et al., 1994; Yokoyama, 2000). This suggests that the *P. melanoleucus* LWS may be considerably blue-shifted relative to the LWS pigment in *Thamnophis* snakes. Within *P. melanoleucus* SWS1, the phenylalanine at site 86 suggests that the pigment will be absorbing in the UV, as is typical of reptilian SWS1 pigments (Hauser et al., 2014). *Pituophis melanoleucus* SWS1, as well as other colubrid SWS1 (Simões et al., 2016), has hydrophobic residues at two spectral tuning sites, A90 and V93. These sites usually have polar or charged amino acid side chains (Carvalho et al., 2011; Hauser et al., 2014). The functional significance of these hydrophobic residues has yet to be characterized, and therefore caution should be taken in applying spectral tuning predictions on squamate SWS1 pigments.

Rhodopsin and rod transducin are expressed in the outer segment of photoreceptors

Because *P. melanoleucus* has an anatomically all-cone retina, we used immunohistochemistry to determine whether both rhodopsin and the rod G protein transducin are expressed in cone photoreceptors. We performed fluorescent immunohistochemistry on the transverse cryosections of the retina of *P. melanoleucus* with the rhodopsin antibody (RET-P1) and a rod-specific transducin antibody (K20). Both antibodies have been previously shown to be selective across a range of vertebrates (Fekete and Barnstable, 1983; Hicks and Barnstable, 1987; Osborne et al., 1999; Schott et al., 2016). We also used these antibodies on a CD1 mouse retina, following similar preparation, as a positive control.

Our results showed rhodopsin localized to the outer segments of select photoreceptors of the *P. melanoleucus* retina (red, Fig. 1D),

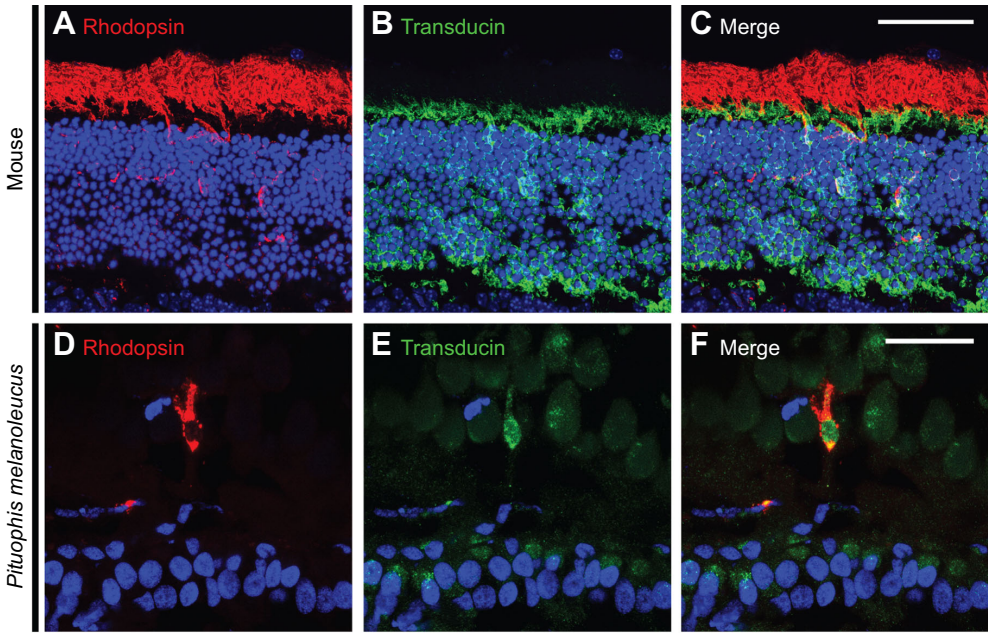

Fig. 1. Fluorescent immunohistochemical staining to localize the presence of rhodopsin and rod transducin in the retina of *P. melanoleucus*, with the rod-dominant mouse retina as a control. Immunohistochemical staining of control (mouse, A–C, scale bar=40 µm) and pine snake (D–F, scale bar=20 µm) transverse retinal cryosections with rhodopsin (RET-P1) and rod-specific-transducin (K20) antibodies. Rhodopsin is found in a subset of cone-like photoreceptors localized to the outer segment (D). Rod-specific transducin is also found in the same photoreceptor, primarily to the inner segment (E). Double staining indicates that both rhodopsin and rod-specific transducin are found within the same cell (F). Nuclei are shown in blue, rhodopsin in red and rod-specific transducin in green.

Journal of Experimental Biology

Journal of Experimental Biology (2017) 220, 2418-2425 doi:10.1242/jeb.156430

whereas the rod transducin localized to the inner segment (green, Fig. 1E). The small amount of colocalization between rhodopsin and transducin in the inner segment (yellow, Fig. 1F) is expected because the animal was not dark-adapted prior to euthanasia, as rod transducin translocates to the inner segment when exposed to bright light (Calvert et al., 2006; Elias et al., 2004). This pattern is consistent with rhodopsin and transducin staining in the *T. proximus* retina (Schott et al., 2016) and the previously unexplained results of rhodopsin detected in the retina of *T. sirtalis* (Sillman et al., 1997).

As expected, CD1 mouse retina had strong rhodopsin fluorescence (red, Fig. 1A) in the outer segment and strong rod transducin staining (green, Fig. 1B) in the inner segment, consistent with the rod-dominant mouse retina. The lack of colocalization is consistent with a light-adapted retina (Calvert et al., 2006; Elias et al., 2004) (Fig. 1C).

Pituophis melanoleucus opsins are all functional *in vitro* with a highly blue-shifted rhodopsin

Complete coding sequences of the *P. melanoleucus* RH1, LWS and SWS1 opsins were cloned into the p1D4-hrGFP II expression vector and transfected into HEK293T cells, and the expressed protein was then purified with the 1D4 monoclonal antibody (Morrow and Chang, 2015; Morrow et al., 2011). Bovine wild-type rhodopsin was used as a control (Fig. 2A). Pine snake rhodopsin has a λ_{max} of 481 nm (Fig. 2B), which is similar to the measured λ_{max} of rhodopsins from *T. proximus*, *T. sirtalis* and *Arizona elegans* snakes (Schott et al., 2016; Sillman et al., 1997; Simões et al., 2016). The drastic blue shift is expected given the presence of the blue-shifting N83 and S292 amino acid identities (Bickelmann et al., 2012; Dungan et al., 2016; van Hazel et al., 2016). *Pituophis melanoleucus* rhodopsin expression was similar to that of *T. proximus*, with a large ratio between total purified protein (absorbance at 280 nm) and active protein (absorbance at λ_{max}) that indicates that only a small proportion of the translated opsin protein is able to bind chromophore and become functionally active. One possible explanation for this effect involves the S185 residue in *P. melanoleucus* rhodopsin, as mutations at this site have been shown to affect the retinal binding efficiency of rhodopsin pigments expressed *in vitro* (McKibbin et al., 2007).

Expression of pine snake SWS1 showed a more typical 280 nm to λ_{max} ratio (Fig. 2C). We found that *P. melanoleucus* SWS1 pigment absorbs in the UV range with a λ_{max} of 370 nm, similar to the SWS1 λ_{max} of *Lampropeltis getula*, *Rhinocheilus lecontei* and *Hypsiglena torquata* (Simões et al., 2016), all of which have the most red-shifted UV SWS measured among colubrid snakes.

Similar to the SWS1 expression, LWS also expressed quite well, with a large proportion of functional pigment (Fig. 2D). Fit to A1 templates gave a λ_{max} of 534 nm, which is blue-shifted relative to

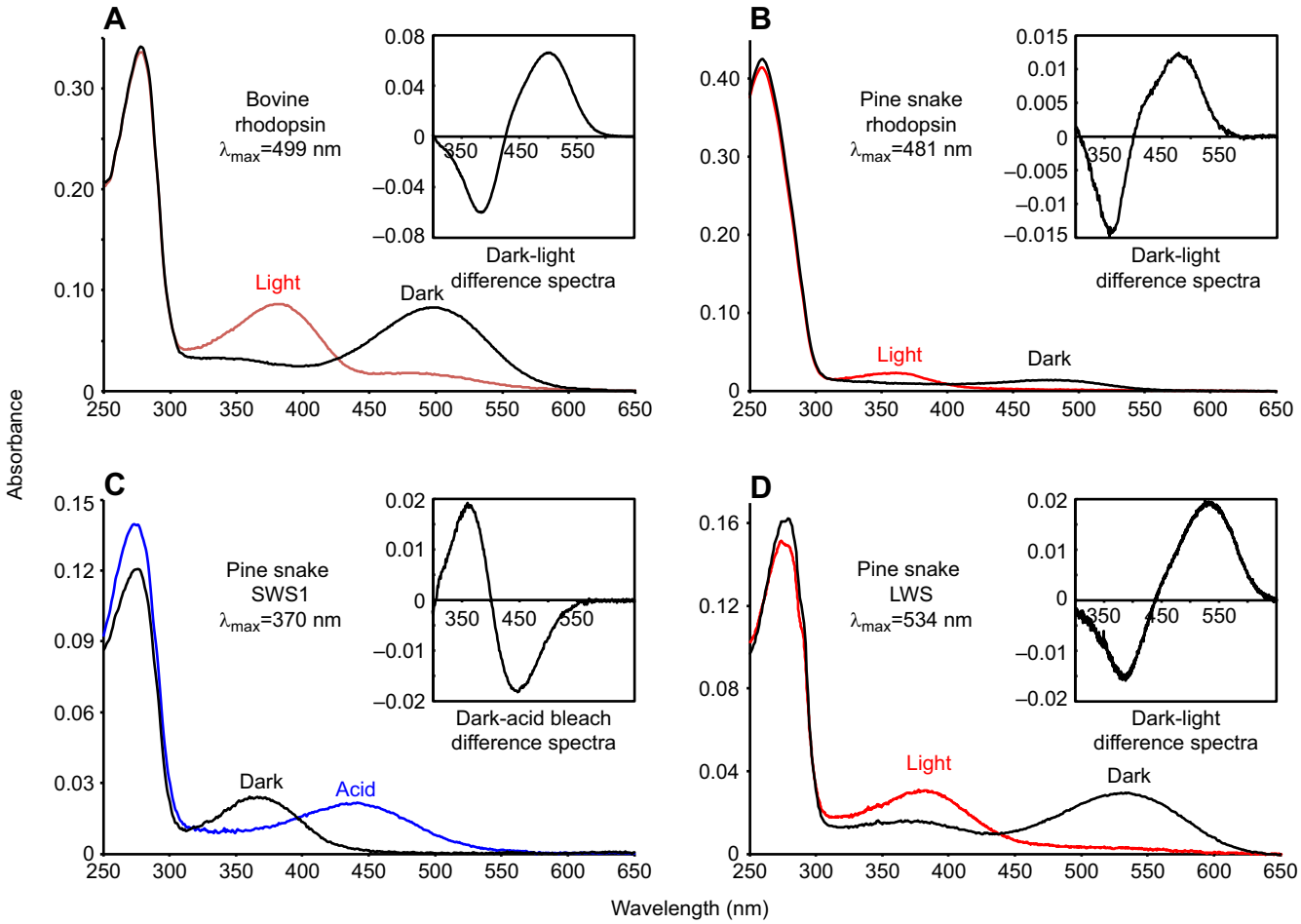

Fig. 2. UV-visible dark absorption spectra of pine snake opsins. (A) Bovine wild-type rhodopsin was used as a control for expressions. Dark spectra for pine snake (B) rhodopsin, (C) SWS1 and (D) LWS. Insets in A, B and D are the dark-light spectra. Inset in C is the dark-acid bleach spectrum. All insets have the same axes as larger spectra. λ_{max} estimations are shown for each pigment.

Journal of Experimental Biology

Journal of Experimental Biology (2017) 220, 2418-2425 doi:10.1242/jeb.156430

Thamnophis (Schott et al., 2016; Sillman et al., 1997), but identical with LWS microspectrophotometric (MSP) measurements of *H. torquata* (Simões et al., 2016) and very close to those of *L. getula*, *A. elegans* and *R. lecontei* (Simões et al., 2016).

Pituophis melanoleucus rhodopsin demonstrates cone opsin-like functional characteristics

In order to confirm the covalent attachment of the chromophore in *P. melanoleucus* SWS1 pigments, the purified opsin was acid bleached (Fig. 2C). We found a shift of the λ_{max} from 370 to 440 nm, which indicates the presence of 11-*cis* retinal covalently bound by a protonated Schiff base to a denatured opsin protein (Kito et al., 1968), suggesting that the UV sensitivity of the pigment may be established by only the presence of F86.

Pituophis melanoleucus LWS (Fig. 3A) and RH1 (Fig. 3B) were tested for hydroxylamine reactivity, which assesses the accessibility of the chromophore-binding pocket to attack by small molecules. If hydroxylamine can enter the binding pocket, it will hydrolyze the Schiff base linkage, resulting in an absorbance decrease of the dark peak and the increase of a retinal oxime peak at 363 nm. Rhodopsins are thought to be largely non-reactive in the presence of hydroxylamine (Dartnall, 1968) (Fig. 3C) because of their highly structured and tightly packed chromophore binding pockets relative to cone opsins, which often react when incubated in hydroxylamine (van Hazel et al., 2013). *Pituophis melanoleucus* LWS reacted to hydroxylamine, as expected, with a reaction half-life ($t_{1/2}$) of ∼3.9 min (Fig. 3A), a time within the range of cone opsins (Das et al., 2004; Ma et al., 2001). As the λ_{max} of *P. melanoleucus* SWS1 is 370 nm, it was not tested as we would not be able to distinguish the retinal oxime peak from the λ_{max} peak. Interestingly, *P. melanoleucus* rhodopsin also reacted to hydroxylamine with a $t_{1/2}$ of ∼14 min (Fig. 3B), unlike the bovine rhodopsin control, which did not react (Fig. 3C). This implies that the chromophore binding pocket of *P. melanoleucus* rhodopsin has a more open configuration relative to other rhodopsin proteins, a property more typical of cone opsins.

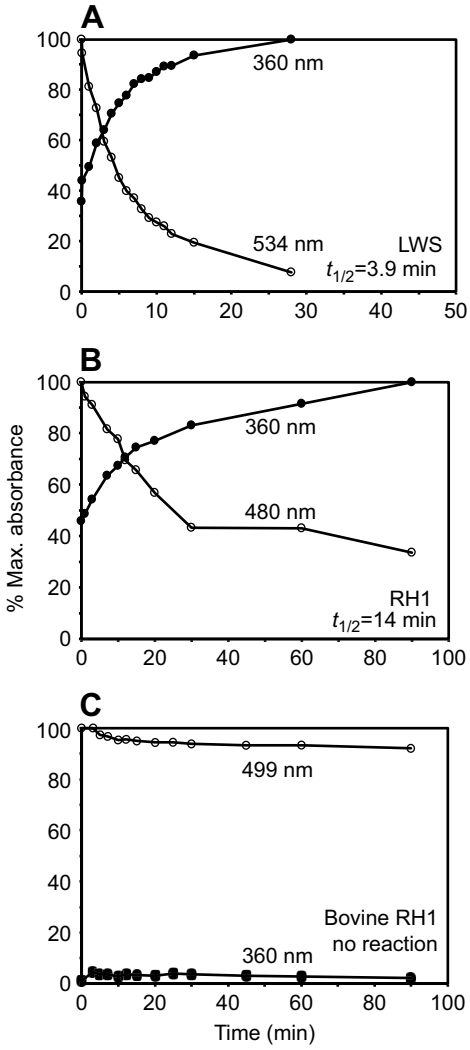

Fig. 3. Comparison of hydroxylamine reactivity of pine snake rod and cone visual pigments with bovine rhodopsin. (A) Pine snake LWS visual pigment, (B) pine snake rhodopsin and (C) bovine rhodopsin. Absorption values of the dark λ_{max} peak decrease over time (open circles), while absorption of the retinal oxime at 360 nm increase over time (solid circles). The half-lives of the reactive opsins were determined via curve fitting exponential rise and decay equations to data.

DISCUSSION

Recently, there has been mounting evidence supporting the theory of transmutation in photoreceptor evolution, proposed by Walls in 1942 (Walls, 1942), which outlines the evolutionary transformation of one photoreceptor type into another in reptilian retinas. Evidence of cone-to-rod transmutation in nocturnal geckos has been extensively demonstrated using both cellular and molecular techniques (Crescitelli, 1956; Dodt and Walther, 1958; Kojima et al., 1992; McDevitt et al., 1993; Röll, 2001; Sakami et al., 2014; Tansley, 1959, 1961, 1964; Zhang et al., 2006), while evidence of rod-to-cone transmutation in colubrid snakes remains somewhat sparse (Schott et al., 2016). In order to demonstrate rod-to-cone transmutation in the retina, there needs to be evidence of a functional rod machinery in a photoreceptor with some rod-like features in a retina that appears, superficially, to consist of only cones. Certainly, the presence of RH1 genes and MSP data suggest transmutation has occurred in several colubrid species (Hart et al., 2012; Sillman et al., 1997; Simões et al., 2015, 2016), but further investigation is required in order to firmly state whether transmutation is present in the retinas of these colubrid snakes, as there are multiple alternate explanations possible (RH1 in the genome but not expressed, rhodopsin expressed but not functional, a cone cell co-opting rhodopsin, etc.). There is only one colubrid snake species for which cellular and molecular evidence for transmutation has been reported: *Thamnophis proximus* (Schott et al., 2016).

The present study provides strong evidence that supports the hypothesis that photoreceptor transmutation has occurred in the retina of *P. melanoleucus*. As *P. melanoleucus* is not closely related to snakes in the genus *Thamnophis*, this suggests that transmutation may be widespread in colubrid snakes. However, the functional significance of transmutation in colubrid snakes still has not been established. In geckos, the advantage of cone-to-rod transmutation is more straightforward as these nocturnal animals are most likely compensating for the loss of RH1 in their diurnal ancestor. We propose that transmutation in colubrids may have occurred as an adaptation to diurnality that provided *P. melanoleucus* with a cone-like rod photoreceptor that operates at brighter light levels, perhaps as a compensation for the loss of the RH2 cone opsins. Our finding of a highly blue-shifted rhodopsin with more cone-like functional properties, as indicated by hydroxylamine reactivity, supports this hypothesis.

Pituophis melanoleucus rhodopsin shows hydroxylamine reactivity, a canonical cone opsin property (Wald et al., 1955). With a reaction half-life of ∼14 min, the *P. melanoleucus* rhodopsin

Journal of Experimental Biology (2017) 220, 2418-2425 doi:10.1242/jeb.156430

reacts much quicker and closer to cone opsin speeds (Das et al., 2004; Ma et al., 2001) than previous rhodopsins that have reacted when incubated in hydroxylamine, such as those of the echidna (Bickelmann et al., 2012) and the anole (Kawamura and Yokoyama, 1998), which react over hours. The RH1 sequence contains both E122 and I189, which are known to mediate the slower decay and regeneration kinetics typical of rhodopsin (Imai et al., 1997; Kuwayama et al., 2002). Conversely, the presence of serine rather than cysteine at site 185 in rhodopsin has been shown to activate fewer G proteins (Karnik et al., 1988), and mutation at site 185 has been shown to reduce the thermal stability of the protein (McKibbin et al., 2007), both characteristics being more typical of cone opsins. Cones have been optimized for fast regeneration, with cone opsin meta-intermediate states being short lived compared with those of rhodopsin (Imai et al., 2005), and a cone-specific Müller cell retinoid cycle (Das et al., 1992) providing a dedicated pool of 11-*cis* retinal. These faster kinetic properties are hypothesized to be facilitated in cone opsins via the relative 'openness' of the chromophore binding pocket, which allows water molecules, and therefore other small molecules such as hydroxylamine, to access the chromophore where they can participate in Schiff base hydrolysis (Chen et al., 2012; Piechnick et al., 2012; Wald et al., 1955). Rhodopsins, in contrast, are optimized for sensitivity and signal amplification; therefore, E122/I189 and a tighter overall structure contribute to a slower active state decay, allowing for the activation of multiple G proteins (Chen et al., 2012; Starace and Knox, 1997), increased thermal stability relative to cone opsins (Barlow, 1964) and a resistance to hydroxylamine (Dartnall, 1968). *Pituophis melanoleucus* rhodopsin shows adaptations to decrease the number of G proteins activated as well as hydroxylamine reactivity, which suggests that an open chromophore binding pocket would enable water access to facilitate active state decay, Schiff base linkage hydrolysis and retinal regeneration (Chen et al., 2012) rates similar to cone opsins. Spectroscopic assays measuring G protein activation and retinal release rates have never been performed on colubrid rhodopsins, but would be an interesting direction for future research characterizing this cone-opsin-like rhodopsin.

Retinal immunohistochemistry localized *P. melanoleucus* rhodopsin protein in the outer segment of an anatomically cone-like photoreceptor, as well as the presence of rod transducin in the inner segment. Rod and cone transducin are thought to originate via duplication from one ancestral gene (Larhammar et al., 2009) and both have been shown to function with all opsins (Sakurai et al., 2007); therefore, the presence and preservation of rod transducin in the photoreceptor supports the theory that this is indeed a transmuted rod and not a cone photoreceptor co-opting rhodopsin expression. Because the retinas were not dark adapted prior to euthanasia, we can presume that under normal photopic light conditions, *P. melanoleucus* rod transducin is cycled out of the outer segment of the cone-like rod, a distinct rod property (Chen et al., 2007; Rosenzweig et al., 2007). In the light, rods cycle transducin and recoverin out of the outer segment, and arrestin into it (Calvert et al., 2006). This allows the rod to effectively shut down phototransduction under bleaching conditions to prevent damage to the photoreceptor. Cones generally do not cycle transducin out of the outer segment of the photoreceptor under normal light conditions (Chen et al., 2007). This suggests that the rhodopsin-expressing photoreceptors in the retina of *P. melanoleucus* would not be able to generate a photoresponse in normal daylight, and thus if this cone-like rod is participating in colour vision with the canonical cones in the retina, it would likely only be under mesopic light conditions where both photoreceptor cell types can be active.

Our microscopy results of the *P. melanoleucus* retina additionally revealed a cone-like rod, which still looks distinct in comparison with the other cones. The cone-like rod outer segment and inner segment had similar diameters with a relatively long outer segment, while the surrounding cones had distinctly large ellipsoids in the inner segment, and proportionally smaller outer segments. Rod photoreceptor morphology is also generally specialized to maximize sensitivity with long cylindrical outer segments (Lamb, 2013). Cone morphological specializations, however, are thought to enable selective colour vision, a faster phototransduction and visual pigment regeneration, while also minimizing metabolic load by miniaturizing the overall structures with large ellipsoids that tunnel light onto smaller tapered outer segments (Hárosi and Novales Flamarique, 2012). A previous study used electron microscopy on the retina of *T. proximus* and showed that the membrane discs unique to rods in the outer segment are still present in the transmuted photoreceptor (Schott et al., 2016). Interestingly, a reduction of RH1 expression levels has been shown to reduce the size of the outer segment of rods, in addition to lowering the photosensitivity and altering the kinetics of the cell to be more cone-like (Makino et al., 2012; Rakshit and Park, 2015; Wen et al., 2009). Currently, the relative expression levels of RH1 in the retinas of colubrid snakes have not been measured. There are additional specializations in the synaptic structures that reflect the different priorities in rod and cone function (Lamb, 2013), but the synaptic structure of the cone-like rod also remains uninvestigated.

Results from this study suggest that transmutation is modifying the function of a subset of photoreceptors in the retina of *P. melanoleucus*. These modifications may serve to lower the sensitivity and signal amplification of the photoreceptor, supporting the hypothesis of a more cone-like function. However, the type of signal these transmuted rods send to the brain is still unknown. Rods and cones are known to have distinct electroretinogram responses, but *T. sirtalis* is the only colubrid snake with electroretinogram measurements performed at a variety of light levels (Jacobs et al., 1992). However, that study did not record any scotopic (rod) response, nor did it record any photopic response from the SWS1-type photoreceptors, which suggests that the results of the study may be incomplete or that the scotopic pathways in the colubrid eye have degraded. Indeed, in high scotopic and mesopic light levels, mammalian rod photoreceptors can and do use cone pathways (Daw et al., 1990; Gregg et al., 2013). And while the presence of amacrine cells has been demonstrated in the duplex retina of turtles (Baylor and Fettiplace, 1977; Walls, 1942) and in the simplex retina of sea snakes (Hibbard and Lavergne, 1972), the presence of rod bipolar cells and AII amacrine cells, both of which are required in the rod-specific photoresponse pathway (Lamb, 2013), has never been established in the colubrid retina.

The evolution of cone-like functionality in a rod photoreceptor may be an attempt to compensate for the loss of the RH2 cone opsin and the lack of spectral overlap between the LWS and SWS1 pigments, such that it could participate in colour vision. In addition to the molecular modifications to *P. melanoleucus* rhodopsin and the physiological modifications to the rod cell, the extreme blue-shift of the RH1 λ_{max}, which is quite rare for terrestrial rhodopsins, may itself be an adaptation for colour vision, as a λ_{max} of ∼480 nm is in the range of typical RH2 pigments (Lamb, 2013). *Pituophis melanoleucus*, in comparison to the *Thamnophis* genera (Schott et al., 2016; Sillman et al., 1997), has a narrower overall range of spectral sensitivities. There could be two possible reasons for this narrowing. It could be that this narrowing of the spectral ranges is to facilitate spectral overlap as an adaptation in *P. melanoleucus*. Or

the narrowing of the spectral range may simply be due to phylogenetic history, as *P. melanoleucus* LWS and SWS1 absorb at similar wavelengths to its closest relatives (Simões et al., 2016), which in turn could be an adaptation, but not one that is due to the specific visual environment of *P. melanoleucus*. Trichromatic vision would be greatly advantageous for a diurnal species (Ankel-Simons and Rasmussen, 2008; Heesy and Ross, 2001), and perhaps sacrificing scotopic vision in order to achieve better mesopic and photopic vision is possible, because other snake sensory systems adaptations, such as chemoreception, could be sufficient in dim light environments (Drummond, 1985). However, currently there is a lack of behavioural studies investigating trichromatic colour discrimination in colubrid snakes under mesopic light conditions.

We hypothesize that rod-to-cone transmutation may be allowing colubrid snakes to have a third cone-like photoreceptor, allowing for spectral sensitivity between SWS1 and LWS, and possibly also trichromatic colour perception in mesopic light conditions. The loss of RH1 in nocturnal geckos and the resulting transmutation of cone into rod demonstrate that the visual system of squamates is capable of adapting to compensate for previous functionality loss in different photoreceptor types. In colubrid snakes, and possibly squamates in general, the rod/cone photoreceptor binary is not as distinct as it is in other vertebrates, and caution should be taken in classifying rod or cone photoreceptors based on limited characterization.

In summary, we find that *P. melanoleucus*, like *T. proximus*, has an all-cone retina derived through evolutionary transmutation of the rod photoreceptors. Furthermore, *P. melanoleucus* rhodopsin is the first vertebrate rhodopsin to show hydroxylamine reactivity similar to cone opsins. This study is also the first to demonstrate the functional effects of transmutation in the retina of colubrid snakes. We suggest that transmutation in colubrid snakes is an adaptation to diurnality and is compensating for the loss of RH2 by establishing spectral sensitivity in a range where the existing SWS1 and LWS are not sensitive, and possibly establishing trichromatic colour vision. Perhaps transmutation in colubrid snakes has contributed to the widespread success of the snake family across such a vast range of ecologies and lifestyle. Ultimately, future work investigating the functional effects of transmutation, from behavioural to molecular, will reveal the significance of rod-to-cone transmutation in colubrid snakes.

Acknowledgements
We thank Dr Rosalie Crouch for generously providing 11-*cis* retinal, and two anonymous reviewers for their feedback and suggestions.

Competing interests
The authors declare no competing or financial interests.

Author contributions
Conceptualization: B.C., N.B.; Methodology: N.B., B.D., R.K.S.; Investigation: B.C., N.B., B.D., R.K.S., V.T.; Resources: B.C., V.T.; Writing - original draft: N.B.; Writing - review & editing: B.C., N.B., R.K.S., V.T.; Visualization: N.B.; Supervision: B.C., V.T.; Project administration: B.C.; Funding acquisition: B.C., V.T.

Funding
This work was supported by a National Sciences and Engineering Research Council of Canada (NSERC) Discovery Grant (to B.S.W.C. and V.T.), a Vision Science Research Program Scholarship (to N.B. and R.K.S.) and an Ontario Graduate Scholarship (to R.K.S.).

Data availability
Pituophis melanoleucus sequences have been deposited in GenBank with the following accession numbers: RH1: MF076667, SWS1: MF076668, LWS: MF076669.

Supplementary information
Supplementary information available online at
http://jeb.biologists.org/lookup/doi/10.1242/jeb.156430.supplemental

References
Ankel-Simons, F. and Rasmussen, D. T. (2008). Diurnality, nocturnality, and the evolution of primate visual systems. *Am. J. Phys. Anthropol.* **137**, 100-117.
Asenjo, A. B., Rim, J. and Oprian, D. D. (1994). Molecular determinants of human red/green color discrimination. *Neuron* **12**, 1131-1138.
Barlow, H. B. (1964). Dark-adaptation: a new hypothesis. *Vision Res.* **4**, 47-58.
Baylor, D. A. and Fettiplace, R. (1977). Transmission from photoreceptors to ganglion cells in turtle retina. *J. Physiol. (Lond.)* **271**, 391-424.
Bickelmann, C., Morrow, J. M., Müller, J. and Chang, B. S. W. (2012). Functional characterization of the rod visual pigment of the echidna (*Tachyglossus aculeatus*), a basal mammal. *Vis. Neurosci.* **29**, 1-7.
Bowmaker, J. K. (2008). Evolution of vertebrate visual pigments. *Vision Res.* **48**, 2022-2041.
Calvert, P. D., Strissel, K. J., Schiesser, W. E., Pugh, E. N., Jr and Arshavsky, V. Y. (2006). Light-driven translocation of signaling proteins in vertebrate photoreceptors. *Trends Cell Biol.* **16**, 560-568.
Caprette, C. L. (2005). *Conquering the Cold Shudder: The Origin and Evolution of Snake Eyes*, pp. 1-122. Ohio: Ohio State University.
Carvalho, L. S., Davies, W. L., Robinson, P. R. and Hunt, D. M. (2011). Spectral tuning and evolution of primate short-wavelength-sensitive visual pigments. *Proc. Biol. Sci.* **279**, rspb20110782-r393.
Chen, J., Wu, M., Sezate, S. A. and McGinnis, J. F. (2007). Light threshold–controlled cone α-transducin translocation. *Invest. Ophthalmol. Vis. Sci.* **48**, 3350-3356.
Chen, M.-H., Kuemmel, C., Birge, R. R. and Knox, B. E. (2012). Rapid release of retinal from a cone visual pigment following photoactivation. *Biochemistry* **51**, 4117-4125.
Cortesi, F., Musilová, Z., Stieb, S. M., Hart, N. S., Siebeck, U. E., Malmstrøm, M., Tørresen, O. K., Jentoft, S., Cheney, K. L., Marshall, N. J. et al. (2015). Ancestral duplications and highly dynamic opsin gene evolution in percomorph fishes. *Proc. Natl. Acad. Sci. USA* **112**, 1493-1498.
Crescitelli, F. (1956). The nature of the gecko visual pigment. *J. Gen. Physiol.* **40**, 217-231.
Dartnall, H. J. A. (1968). The photosensitivities of visual pigments in the presence of hydroxylamine. *Vision Res.* **8**, 339-358.
Das, S. R., Bhardwaj, N., Kjeldbye, H. Gouras, P. (1992). Muller cells of chicken retina synthesize 11-cis-retinol. *Biochem. J.* **285**, 907-913.
Das, J., Crouch, R. K., Ma, J.-X., Oprian, D. D. and Kono, M. (2004). Role of the 9-methyl group of retinal in cone visual pigments. *Biochemistry* **43**, 5532-5538.
Davies, W. L., Cowing, J. A., Bowmaker, J. K., Carvalho, L. S., Gower, D. J. and Hunt, D. M. (2009). Shedding light on serpent sight: the visual pigments of henophidian snakes. *J. Neurosci.* **29**, 7519-7525.
Daw, N. W., Jensen, R. J. and Brunken, W. J. (1990). Rod pathways in mammalian retinae. *Trends Neurosci.* **13**, 110-115.
Diller, L. V. and Wallace, R. L. (1996). Comparative ecology of two snake species (*Crotalus viridis* and *Pituophis melanoleucus*) in Southwestern Idaho. *Herpetologica* **52**, 343-360.
Dodt, E. and Walther, J. B. (1958). *[Spectral sensitivity and the threshold of gecko eyes; electroretinographical studies on Hemidactylus turcicus & Tarentola mauritanica.]. Pflugers Arch.* **268**, 204-212.
Drummond, H. (1985). The role of vision in the predatory behaviour of natricine snakes. *Anim. Behav.* **33**, 206-215.
Dungan, S. Z., Kosyakov, A. and Chang, B. S. W. (2016). Spectral tuning of killer whale (*Orcinus orca*) rhodopsin: evidence for positive selection and functional adaptation in a cetacean visual pigment. *Mol. Biol. Evol.* **33**, 323-336.
Edgar, R. C. (2004). MUSCLE: multiple sequence alignment with high accuracy and high throughput. *Nucleic Acids Res.* **32**, 1792-1797.
Elias, R. V., Sezate, S. S., Cao, W. and McGinnis, J. F. (2004). Temporal kinetics of the light/dark translocation and compartmentation of arrestin and alpha-transducin in mouse photoreceptor cells. *Mol. Vis.* **10**, 672-681.
Fekete, D. M. and Barnstable, C. J. (1983). The subcellular localization of rat photoreceptor-specific antigens. *J. Neurocytol.* **12**, 785-803.
Gerald, G. W., Bailey, M. A. and Holmes, J. N. (2006). Movements and activity range sizes of northern pinesnakes (*Pituophis melanoleucus melanoleucus*) in Middle Tennessee. *J. Herpetol.* **40**, 503-510.
Govardovskii, V. I., Fyhrquist, N., Reuter, T., Kuzmin, D. G. and Donner, K. (2000). In search of the visual pigment template. *Vis. Neurosci.* **17**, 509-528.
Gregg, R. G., McCall, M. A. and Massey, S. C. (2013). Function and anatomy of the mammalian retina. In *Retina*, 5th edn, Vol. 1, pp. 360-400. Amsterdam: Elsevier Inc.
Hárosi, F. I. and Novales Flamarique, I. (2012). Functional significance of the taper of vertebrate cone photoreceptors. *J. Gen. Physiol.* **139**, 159-187.
Hart, N. S., Coimbra, J. P., Collin, S. P. and Westhoff, G. (2012). Photoreceptor types, visual pigments, and topographic specializations in the retinas of hydrophiid sea snakes. *J. Comp. Neurol.* **520**, 1246-1261.

Hauser, F. E., van Hazel, I. and Chang, B. S. W. (2014). Spectral tuning in vertebrate short wavelength-sensitive 1 (SWS1) visual pigments: can wavelength sensitivity be inferred from sequence data? *J. Exp. Zool. B Mol. Dev. Evol.* **322**, 529-539.
Heesy, C. P. and Ross, C. F. (2001). Evolution of activity patterns and chromatic vision in primates: morphometrics, genetics and cladistics. *J. Hum. Evol.* **40**, 111-149.
Hibbard, E. and Lavergne, J. (1972). Morphology of the retina of the sea-snake, *Pelamis platurus*. *J. Anat.* **112**, 125-136.
Hicks, D. and Barnstable, C. J. (1987). Different rhodopsin monoclonal antibodies reveal different binding patterns on developing and adult rat retina. *J. Histochem. Cytochem.* **35**, 1317-1328.
Himes, J. G. (2001). Burrowing ecology of the rare and elusive Louisiana pine snake, *Pituophis ruthveni* (Serpentes : Colubridae). *Amphib-Reptilia* **22**, 91-101.
Imai, H., Kojima, D., Oura, T., Tachibanaki, S., Terakita, A. and Shichida, Y. (1997). Single amino acid residue as a functional determinant of rod and cone visual pigments. *Proc. Natl. Acad. Sci. USA* **94**, 2322-2326.
Imai, H., Kuwayama, S., Onishi, A., Morizumi, T., Chisaka, O. and Shichida, Y. (2005). Molecular properties of rod and cone visual pigments from purified chicken cone pigments to mouse rhodopsin in situ. *Photochem. Photobiol. Sci.* **4**, 667-668.
Jacobs, G. H., Fenwick, J. A., Crognale, M. A. and Deegan, J. F.II (1992). The all-cone retina of the garter snake: spectral mechanisms and photopigment. *J. Comp. Physiol. A Neuroethol. Sens. Neural. Behav. Physiol.* **170**, 701-707.
Karnik, S. S. and Khorana, H. G. (1990). Assembly of functional rhodopsin requires a disulfide bond between cysteine residues 110 and 187. *J. Biol. Chem.* **265**, 17520-17524.
Karnik, S. S., Sakmar, T. P., Chen, H. B. and Khorana, H. G. (1988). Cysteine residues 110 and 187 are essential for the formation of correct structure in bovine rhodopsin. *Proc. Natl. Acad. Sci. USA* **85**, 8459-8463.
Kawamura, S. and Yokoyama, S. (1998). Functional characterization of visual and nonvisual pigments of American chameleon (*Anolis carolinensis*). *Vision Res.* **38**, 37-44.
Kito, Y., Suzuki, T., Azuma, M. and Sekoguti, Y. (1968). Absorption spectrum of rhodopsin denatured with acid. *Nature* **218**, 955-957.
Kojima, D., Okano, T., Fukada, Y., Shichida, Y., Yoshizawa, T. and Ebrey, T. G. (1992). Cone visual pigments are present in gecko rod cells. *Proc. Natl. Acad. Sci. USA* **89**, 6841-6845.
Kuwayama, S., Imai, H., Hirano, T., Terakita, A. and Shichida, Y. (2002). Conserved proline residue at position 189 in cone visual pigments as a determinant of molecular properties different from rhodopsins. *Biochemistry*. **41**, 15245-15252.
Lamb, T. D. (2013). Progress in retinal and eye research. *Prog. Retin. Eye Res.* **36**, 52-119.
Larhammar, D., Nordström, K. and Larsson, T. A. (2009). Evolution of vertebrate rod and cone phototransduction genes. *Philos. Trans. R. Soc. Lond. B Biol. Sci.* **364**, 2867-2880.
Ma, J. X., Kono, M., Xu, L., Das, J., Ryan, J. C., Hazard, E. S., Oprian, D. D. and Crouch, R. K. (2001). Salamander UV cone pigment: sequence, expression, and spectral properties. *Vis. Neurosci.* **18**, 393-399.
Makino, C. L., Wen, X.-H., Michaud, N. A., Covington, H. I., DiBenedetto, E., Hamm, H. E., Lem, J. and Caruso, G. (2012). Rhodopsin expression level affects rod outer segment morphology and photoresponse kinetics. *PLoS ONE* **7**, e37832-e7.
McDevitt, D. S., Brahma, S. K., Jeanny, J.-C. and Hicks, D. (1993). Presence and foveal enrichment of rod opsin in the 'all cone' retina of the American chameleon. *Anat. Rec.* **237**, 299-307.
McKibbin, C., Toye, A. M., Reeves, P. J., Khorana, H. G., Edwards, P. C., Villa, C. and Booth, P. J. (2007). Opsin stability and folding: the role of Cys185 and abnormal disulfide bond formation in the intradiscal domain. *J. Mol. Biol.* **374**, 1309-1318.
Molday, R. S. and MacKenzie, D. (1983). Monoclonal antibodies to rhodopsin: characterization, cross-reactivity, and application as structural probes. *Biochemistry* **22**, 653-660.
Morrow, J. M. and Chang, B. S. W. (2010). The p1D4-hrGFP II expression vector: a tool for expressing and purifying visual pigments and other G protein-coupled receptors. *Plasmid* **64**, 162-169.
Morrow, J. M. and Chang, B. S. W. (2015). Comparative mutagenesis studies of retinal release in light-activated zebrafish rhodopsin using fluorescence spectroscopy. *Biochemistry* **54**, 4507-4518.
Morrow, J. M., Lazic, S. and Chang, B. S. W. (2011). A novel rhodopsin-like gene expressed in zebrafish retina. *Vis. Neurosci.* **28**, 325-335.
Osborne, N. N., Safa, R. and Nash, M. S. (1999). Photoreceptors are preferentially affected in the rat retina following permanent occlusion of the carotid arteries. *Vision Res.* **39**, 3995-4002.
Palczewski, K., Kumasaka, T., Hori, T., Behnke, C. A., Motoshima, H., Fox, B. A., Le Trong, I., Teller, D. C., Okada, T., Stenkamp, R. E. et al. (2000). Crystal structure of rhodopsin: a G protein-coupled receptor. *Science* **289**, 739-745.
Piechnick, R., Ritter, E., Hildebrand, P. W., Ernst, O. P., Scheerer, P., Hofmann, K. P. and Heck, M. (2012). Effect of channel mutations on the uptake and release of the retinal ligand in opsin. *Proc. Natl. Acad. Sci. USA* **109**, 5247-5252.
Rakshit, T. and Park, P. S.-H. (2015). Impact of reduced rhodopsin expression on the structure of rod outer segment disc membranes. *Biochemistry* **54**, 2885-2894.
Röll, B. (2001). Gecko vision –retinal organization, foveae and implications for binocular vision. *Vision Res.* **41**, 2043-2056.
Ronquist, F. and Huelsenbeck, J. P. (2003). MrBayes 3: bayesian phylogenetic inference under mixed models. *Bioinformatics* **19**, 1572-1574.
Rosenzweig, D. H., Nair, K. S., Wei, J., Wang, Q., Garwin, G., Saari, J. C., Chen, C.-K., Smrcka, A. V., Swaroop, A., Lem, J. et al. (2007). Subunit dissociation and diffusion determine the subcellular localization of rod and cone transducins. *J. Neurosci.* **27**, 5484-5494.
Sakami, S., Kolesnikov, A. V., Kefalov, V. J. and Palczewski, K. (2014). P23H opsin knock-in mice reveal a novel step in retinal rod disc morphogenesis. *Hum. Mol. Genet.* **23**, 1723-1741.
Sakmar, T. P., Franke, R. R. and Khorana, H. G. (1989). Glutamic acid-113 serves as the retinylidene Schiff base counterion in bovine rhodopsin. *Proc. Natl. Acad. Sci. USA* **86**, 8309-8313.
Sakmar, T. P., Menon, S. T., Marin, E. P. and Awad, E. S. (2002). Rhodopsin: insights from recent structural studies. *Annu. Rev. Biophys. Biomol. Struct.* **31**, 443-484.
Sakurai, K., Onishi, A., Imai, H., Chisaka, O., Ueda, Y., Usukura, J., Nakatani, K. and Shichida, Y. (2007). Physiological properties of rod photoreceptor cells in green-sensitive cone pigment knock-in mice. *J. Gen. Physiol.* **130**, 21-40.
Schott, R. K., Müller, J., Yang, C. G. Y., Bhattacharyya, N., Chan, N., Xu, M., Morrow, J. M., Ghenu, A.-H., Loew, E. R., Tropepe, V. et al. (2016). Evolutionary transformation of rod photoreceptors in the all-cone retina of a diurnal garter snake. *Proc. Natl. Acad. Sci. USA* **113**, 356-361.
Sillman, A. J., Govardovskii, V. I., Röhlich, P., Southard, J. A. and Loew, E. R. (1997). The photoreceptors and visual pigments of the garter snake (*Thamnophis sirtalis*): a microspectrophotometric, scanning electron microscopic and immunocytochemical study. *J. Comp. Physiol. A* **181**, 89-101.
Sillman, A. J., Johnson, J. L. and Loew, E. R. (2001). Retinal photoreceptors and visual pigments in *Boa constrictor imperator*. *J. Exp. Zool.* **290**, 359-365.
Simões, B. F., Sampaio, F. L., Jared, C., Antoniazzi, M. M., Loew, E. R., Bowmaker, J. K., Rodriguez, A., Hart, N. S., Hunt, D. M., Partridge, J. C. et al. (2015). Visual system evolution and the nature of the ancestral snake. *J. Evol. Biol.* **28**, 1309-1320.
Simões, B. F., Sampaio, F. L., Loew, E. R., Sanders, K. L., Fisher, R. N., Hart, N. S., Hunt, D. M., Partridge, J. C. and Gower, D. J. (2016). Multiple rod–cone and cone–rod photoreceptor transmutations in snakes: evidence from visual opsin gene expression. *Proc. Biol. Sci.* **283**, 20152624-8.
Starace, D. M. and Knox, B. E. (1997). Activation of transducin by a *Xenopus* short wavelength visual pigment. *J. Biol. Chem.* **272**, 1095-1100.
Stull, O. G. (1940). *Variations and Relationship in the Snake of the Genus Pituophis*. *Washington*, DC, United States: National Museum. Smithsonian Institution. Bulletin.
Taniguchi, Y., Hisatomi, O., Yoshida, M. and Tokunaga, F. (1999). Evolution of visual pigments in geckos. *FEBS Lett.* **445**, 36-40.
Tansley, K. (1959). The retina of two nocturnal geckos *Hemidactylus turcicus* and *Tarentola mauritanica*. *Pflugers Arch. Gesamte Physiol. Menschen Tiere* **268**, 213-220.
Tansley, K. (1961). The retina of a diurnal gecko, *Phelsuma madagascariensis longinsulae*. *Pflugers Arch. Gesamte Physiol. Menschen Tiere* **272**, 262-269.
Tansley, K. (1964). The gecko retina. *Vision Res.* **4**, I33-IN14.
Underwood, G. (1970). The eye. In *Biology of the Reptilia*, Vol. i (ed. C. Gans), pp.1-97. New York: Academic Press.
van Hazel, I., Sabouhanian, A., Day, L., Endler, J. A. and Chang, B. S. W. (2013). Functional characterization of spectral tuning mechanisms in the great bowerbird short-wavelength sensitive visual pigment (SWS1), and the origins of UV/violet vision in passerines and parrots. *BMC Evol. Biol.* **13**, 250.
van Hazel, I., Dungan, S. Z., Hauser, F. E., Morrow, J. M., Endler, J. A. and Chang, B. S. W. (2016). A comparative study of rhodopsin function in the great bowerbird (*Ptilonorhynchus nuchalis*): spectral tuning and light-activated kinetics. *Protein Sci.* **25**, 1308-1318.
Wald, G., Brown, P. K. and Smith, P. H. (1955). Iodopsin. *J. Gen. Physiol.* **38**, 623-681.
Walls, G. L. (1942). *The vertebrate eye and its adaptive radiation [by] Gordon Lynn Walls*. Bloomfield Hills, MI: Cranbrook Institute of Science.
Wen, X.-H., Shen, L., Brush, R. S., Michaud, N., Al-Ubaidi, M. R., Gurevich, V. V., Hamm, H. E., Lem, J., DiBenedetto, E., Anderson, R. E. et al. (2009). Overexpression of rhodopsin alters the structure and photoresponse of rod photoreceptors. *Biophys. J.* **96**, 939-950.
Yokoyama, S. (2000). Molecular evolution of vertebrate visual pigments. *Prog. Retin. Eye Res.* **19**, 385-419.
Zhang, X., Wensel, T. G. and Yuan, C. (2006). Tokay gecko photoreceptors achieve rod-like physiology with cone-like proteins. *Photochem. Photobiol.* **82**, 1452.

Supplemental Information

Table S1. Degenerate Primers designed for sequencing opsin genes from genomic DNA

Opsin	Primer	Sequence (5'-3')	Source
RH1	SquamR1_1F	AAGGAGTCTGARTCIACICARAARGC	This paper
RH1	SquamR1_972R	GCGGAACTGTCGATTCATRAAIACRTADAT	This paper
LWS	DIAPLMF1	AAGCGTATTYAYTTAYACCRACASCAACAA	Davis et al., 2009
LWS	DIAPLMR1	CATCCTBGACACYTCCYTCTCVGCCTTCTG'	Davis et al., 2009
LWS	PM_LWS3'GW_877F	TCTGGCAGCTTCCCTGCCTGCCTTCTT	This paper
LWS	PM_LWS3'GW_877FR	GTAATACGACTCACTATAGGGC	This paper
LWS	PM_LWS3'GW_865F	TGCCTTTCACCCTCTGGCAGCTTCCCT	This paper
LWS	PM_LWS3'GW_865FR	GTAATACGACTCACTATAGGGC	This paper
LWS	PM_LWS3'GW_905F	GCAAAAAGCGCCACCATTTACAACCCA	This paper
LWS	PM_LWS3'GW_905FR	CGGGCTGGTGCGGAACTGTCGATTCAT	This paper
LWS	PM_LWS3'GW_936F	TATACGTCTTCATGAATCGACAGTCCG	This paper
LWS	PM_LWS3'GW_936FR	ACTATAGGGCACGCGTGGT	This paper
LWS	PM_LWS5'GW_212R	GTAATACGACTCACTATAGGGC	This paper
LWS	PM_LWS5'GW_212RR	TTGGCTGTGGCCACCAATACCAAACCA	This paper
LWS	PM_LWS5'GW_210R	GTAATACGACTCACTATAGGGC	This paper
LWS	PM_LWS5'GW_210RR	GGCTGTGGCCACCAATACCAAACCATT	This paper
LWS	PM_LWS5'GW_90R	GTAATACGACTCACTATAGGGC	This paper
LWS	PM_LWS5'GW_90RR	AGGGTCACGGGTATTGTTGCTGTTGGT	This paper
LWS	PM_LWS5'GW_89R	GTAATACGACTCACTATAGGGC	This paper
LWS	PM_LWS5'GW_89RR	GGGTCACGGGTATTGTTGCTGTTGGTG	This paper
SWS1	SquamS1_84F	TCCTCGCCTTCGAACGATATRTSGTSATCT	This paper
SWS1	SquamS1_857R	CATCATCCACTTTYTTSCCRAASAGCTGCA	This paper
SWS1	PM_S13'GW_478F	ATGTACATGGTGAACAACCCTCAGCAC	This paper
SWS1	PM_S13'GW_478FR	GTAATACGACTCACTATAGGGC	This paper
SWS1	PM_S13'GW_477F	CATGTACATGGTGAACAACCCTCAGCA	This paper
SWS1	PM_S13'GW_477FR	GTAATACGACTCACTATAGGGC	This paper
SWS1	PM_S13'GW_519F	CTTGGTCACCATCCCTGCCTTCTTC	This paper
SWS1	PM_S13'GW_519FR	GTAATACGACTCACTATAGGGC	This paper
SWS1	PM_S13'GW_522F	GGTCACCATCCCTGCCTTCTTCTCCAA	This paper
SWS1	PM_S13'GW_522FR	ACTATAGGGCACGCGTGGT	This paper
SWS1	PM_S15'GW_128R	GTAATACGACTCACTATAGGGC	This paper
SWS1	PM_S15'GW_128RR	ACTACCACAGCATGTTTGGAGTGGAAA	This paper
SWS1	PM_S15'GW_120R	GTAATACGACTCACTATAGGGC	This paper
SWS1	PM_S15'GW_120RR	AGCATGTTTGGAGTGGAAACGGAAGT	This paper
SWS1	PM_S15'GW_99R	ACTATAGGGCACGCGTGGT	This paper
SWS1	PM_S15'GW_99RR	GAAGTTCCCCAGCGGCTTGCAGATCAC	This paper
SWS1	PM_S15'GW_95R	ACTATAGGGCACGCGTGGT	This paper
SWS1	PM_S15'GW_95RR	TTCCCCAGCGGCTTGCAGATCACGATA	This paper

Table S2. List of sequences used in the phylogenetic analyses of opsin genes

	RH1	LWS	SWS
Amerotyphlops brongersmianus	KR336737	------	------
Amphisbaena alba	KR336729	KR336705	KR336720
Amphisbaena infraorbitale	KR336730	KR336704	KR336719
Anilius scytale	KR336736	------	------
Anolis carolinensis	NM_001291387	U08131 XM_008103916	AF134194
Arizona elegans	KU324006	KU323986	KU323997
Atractus flammigerus	KR336740	KR336712	KR336726
Bachia flavescens	KR336731	KR336703	KR336715
Epictia collaris	KR336735	------	------
Feylinia	KR336742	KR336714	KR336717
Gekko gecko	------	M92036	AY024356
Gekko japonicus	------	XM_015415465	XM_015427348
Hydrophis peronii	KU324001	KU323990	KU323991
Hypsiglena jani	KU324007	KU323988	KU323998
Iguana iguana	------	------	AB626972
Lampropeltis californiae	KU324004	KU323987	KU323992
Liotyphlops beui	KR336734	------	------
Melanoseps occidentalis	KR336743	KR336713	KR336718
Natrix maura	KU324002	KU323982	KU323993
Notechis scutatus	KU324000	KU323989	KU323999
Ophiodes striatus	KR336732	KR336708	KR336716
Phelsuma madagascariensis	------	AF074043	AF074045
Phyllorhynchus decurtatus	------	KU323985	KU323996
Pituophis melanoleucus	xxxxxx	xxxxxx	xxxxxx
Polemon collaris	KR336739	KR336710	KR336724
Protobothrops mucrosquamatus	XM_015823472	XM_015812260	XM_015825841
Pseustes poecilonotus	KR336741	KR336711	KR336725
Python bivittatus	XM_007423262	XM_007420519	XM_007441636
Python regius	FJ497236	FJ497238	FJ497237
Takydromus sexlineatus	KR336727	KR336707	KR336722
Telescopus fallax	KU324005	KU323984	KU323995
Thamnophis proximus	KU306726	KU306727	KU306728

Thamnophis sirtalis	XM_014059138	XM_014068735	XM_014075668 KU32399
Tropidophis feicki	KR336738	KR336709	KR336723
Typhlophis squamosus	KR336733	------	------
Uta stansburiana	DQ100323	DQ129869	DQ100325
Xenopeltis unicolor	FJ497233	FJ497235	FJ497234

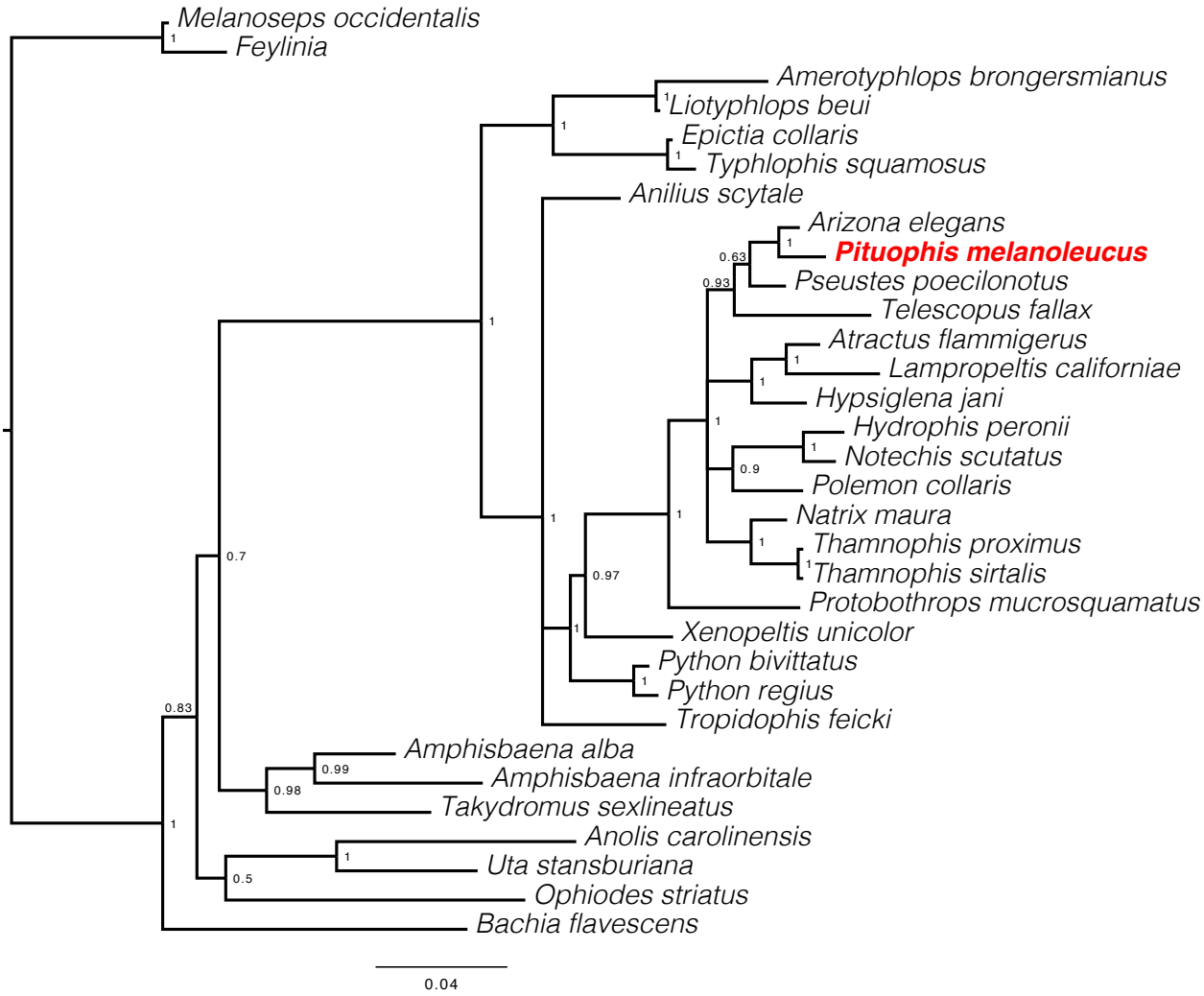

Figure S1. Rhodopsin gene tree estimated using Bayesian inference illustrating the position of *Pituophis melanoleucus* RH1. Numbers at the nodes are posterior probability percentages.

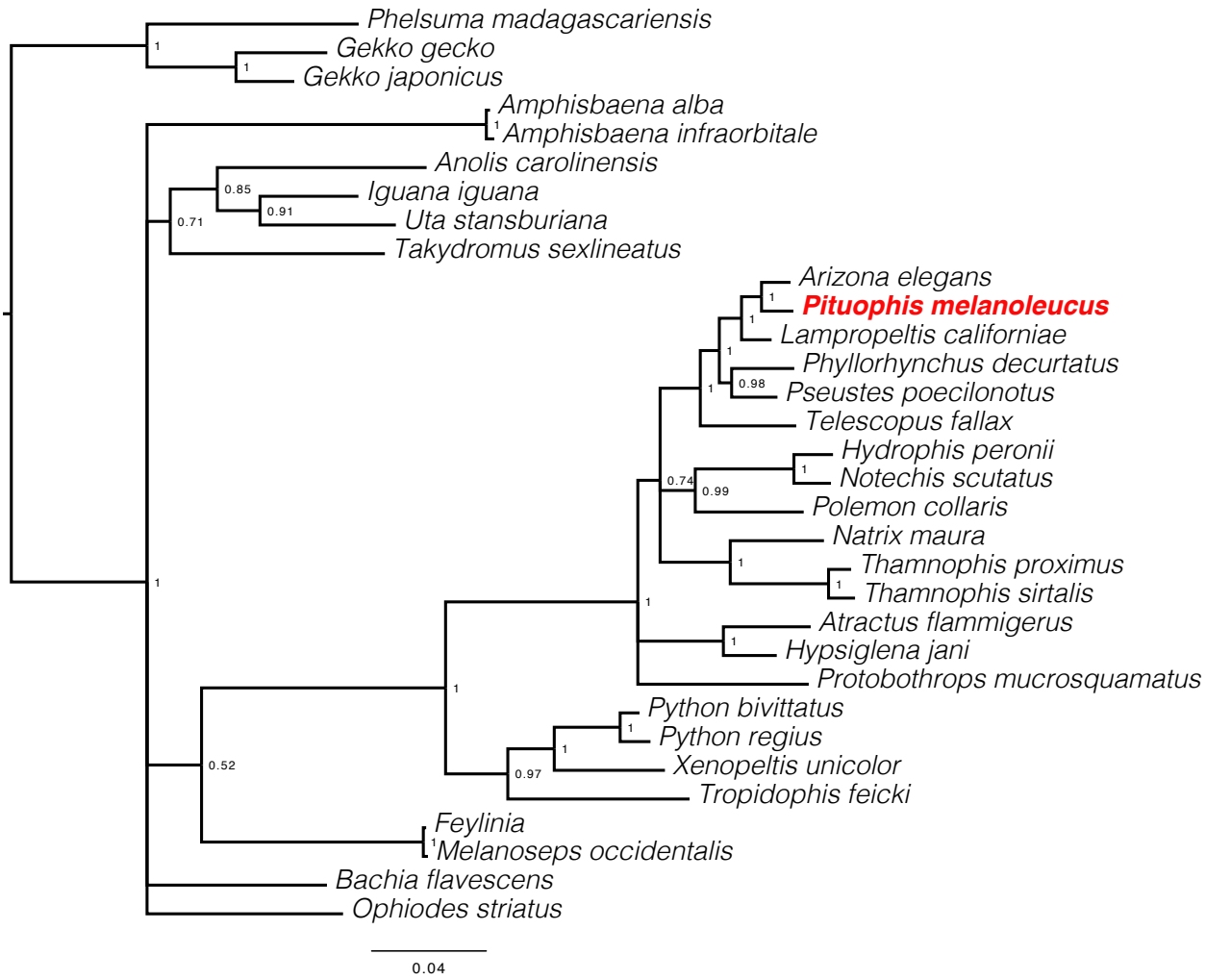

Figure S2. SWS1 gene tree estimated using Bayesian inference illustrating the position of *Pituophis melanoleucus* SWS1. Numbers at the nodes are posterior probability percentages.

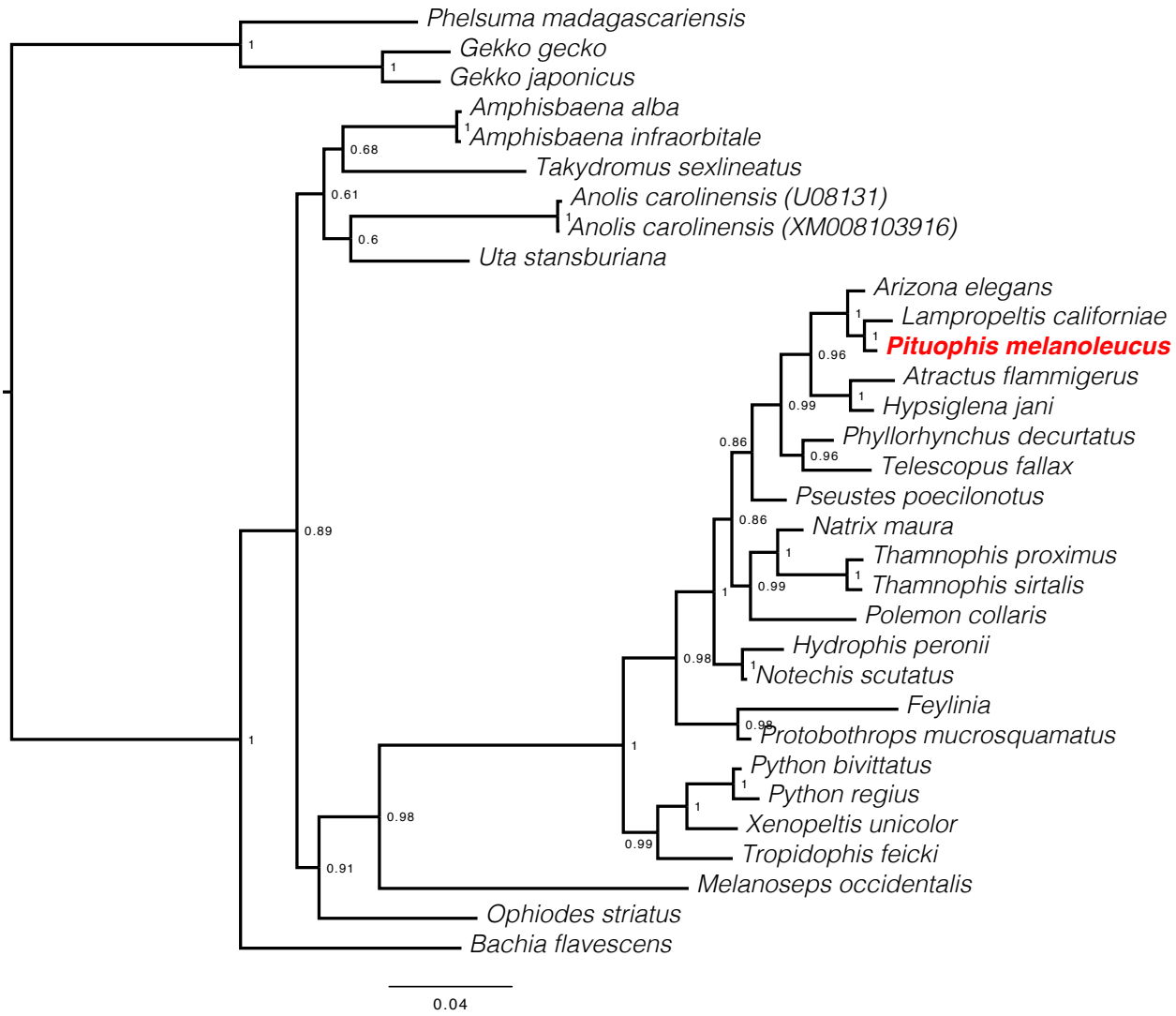

Figure S3. LWS gene tree estimated using Bayesian inference illustrating the position of *Pituophis melanoleucus* LWS. Numbers at the nodes are posterior probability percentages.